Cell, Vol. 89, 1121–1132, June 27, 1997, Copyright ©1997 by Cell Press

Regulation of IRK3 Inward Rectifier K^+ Channel by m1 Acetylcholine Receptor and Intracellular Magnesium

Huai-hu Chuang, Yuh Nung Jan, and Lily Yeh Jan*
Departments of Physiology and Biochemistry
Howard Hughes Medical Institute
University of California
San Francisco, California 94143-0724

Summary

Inward rectifier K^+ channels control the cell's membrane potential and neuronal excitability. We report that the IRK3 but not the IRK1 inward rectifier K^+ channel activity is inhibited by m1 muscarinic acetylcholine receptor. This m1 modulation cannot be accounted for by protein kinase C, Ca^{2+}, or channel phosphorylation, but can be mimicked by Mg^{2+}. Based on quantitative analyses of IRK3 and two different IRK1 mutant channels bestowed with sensitivity to m1 modulation, we suggest that the resting Mg^{2+} level causes chronic inhibition of IRK3 channels, and m1 receptor stimulation may lead to an increase of cytoplasmic Mg^{2+} concentration and further channel inhibition, due to the ability of Mg^{2+} to lead these channels into a prolonged inactivated state.

Introduction

In the central nervous system, many neurotransmitters activate receptors coupled to G proteins. The second messengers generated by receptor stimulation then act upon effectors, including inward rectifier K^+ channels that contribute to the determination of the resting membrane potential and the membrane input resistance (Hille, 1992). Modulation of these K^+ channels can thus alter the membrane potential, the frequency of action potentials, and temporal–spatial summation of impinging signals, leading to regulation of heart rate, information processing, and secretion of hormones, neurotransmitters, or enzymes (DiFrancesco et al., 1980; Sakmann et al., 1983; Noble, 1984; Soejima and Noma, 1984; Dukes and Philipson, 1996).

Regulation of inward rectifier K^+ channels by inhibitory transmitters may involve direct action of the G-protein subunits. In the case of channel activation by the m2 acetylcholine receptor (m2 AChR) in the cardiac cells (Sakmann et al., 1983; Soejima and Noma, 1984; Kurachi et al., 1986; Wickman et al., 1994) or by inhibitory neurotransmitter receptors in central neurons (Egan and North, 1986; North et al., 1987; Inoue et al., 1988; Oh et al., 1995; Velimirovic et al., 1995), channel activation is fast, within tens of milliseconds of transmitter action (Hille, 1992; Sodickson and Bean, 1996), and is mediated by pertussis toxin–sensitive G proteins, probably due to the direct action of the $G\beta\gamma$ subunit (Reuveny et al., 1994; Yamada et al., 1994; Huang et al., 1995; Kofuji et al., 1995; Krapivinsky et al., 1995; Kunkel and Peralta, 1995).

In contrast, excitatory neurotransmitters may cause suppression of inward rectifier K^+ channel activities in central neurons (Stanfield et al., 1985; Nakajima et al., 1988; North and Uchimura, 1989; Shen and North, 1992; Velimirovic et al., 1995). Substance P causes a slow excitation in nucleus basalis neurons by inhibiting inward rectifier K^+ channel activities via pertussis toxin–insensitive G proteins (Takano et al., 1995). Similar channel modulation is mediated by serotonin and acetylcholine, likely through 5-HT_2 receptors and m1 acetylcholine receptors (m1 AChR), respectively, in nucleus accumbens neurons (North and Uchimura, 1989; Uchimura and North, 1990), and by m1 AChR in the rat sympathetic ganglia (Wang and McKinnon, 1996). These transmitter actions usually entail a long latency, ranging from tens of milliseconds to minutes, before the onset of channel inhibition. The inhibition tends to last for minutes.

Inhibition of inward rectifier K^+ channels is often mediated by transmitter receptors coupled to pertussis toxin–insensitive G proteins, probably $G_{q/11}$, which are known to activate phospholipase C (PLC) and downstream second messengers such as diacylglycerol (DAG), inositol-trisphosphate (IP_3), protein kinase C (PKC), and arachidonic acid (AA) (Peralta et al., 1988; Caulfield, 1993; Huang et al., 1993). The mechanism for channel inhibition, however, is not always understood. In nucleus basalis neurons, a PKC inhibitor occludes the modulatory action of substance P (Takano et al., 1995). In cardiac cells, α1 inhibition of inward rectifier K^+ current persists in the presence of the kinase inhibitors H-7 and staurosporine, and cannot be abolished by down-regulation of PKC (Braun et al., 1992). However, direct application of PKC to the excised membrane patch inhibits the K^+ channels (Sato and Koumi, 1995). As for other channels modulated by these transmitter receptors, transmitter action in chick dorsal root ganglion leads to activation of G_o, PLC, DAG, and PKC, and subsequent depression of Ca^{2+} current (Rane et al., 1989). In the sympathetic ganglia, LHRH, substance P, and muscarinic agonists inhibit the M-type K^+ channels (Robbins et al., 1993; Caulfield et al., 1994; Jones et al., 1995). This inhibition is not mediated by cyclic AMP, cyclic GMP, PKC, or AA, but may involve the action of Ca^{2+} (Marrion, 1996; Selyanko and Brown, 1996).

In this study, we expressed IRK3 (Kir2.3) (Morishige et al., 1994; Perier et al., 1994; Collins et al., 1996), one member of the inward rectifier K^+ channel family, in Xenopus laevis oocytes. We found that IRK3 channels are inhibited by m1 AChR stimulation, due to the action of a novel diffusible cytoplasmic factor. Moreover, roughly half of the IRK3 channels in oocytes or mammalian cells are inhibited without m1 AChR stimulation. This chronic inhibition is accounted for by a voltage-independent Mg^{2+} inhibition different from the Mg^{2+} block of the inward rectifier K^+ channel pore. Having performed several tests on the possibility that this Mg^{2+} inhibition also underlies the m1 AChR-induced channel

*To whom correspondence and communication should be addressed.

inhibition, we conclude that Mg^{2+}, or a factor that behaves like Mg^{2+} in these tests, mediates this m1 modulation of inward rectifier K^+ channels.

Results

IRK3 Is Modulated by m1AChR

Inward rectifier K^+ currents were recorded via a two-electrode voltage clamp from Xenopus oocytes injected with in vitro–transcribed cRNAs for IRK3 and m1 AChR. A substantial amount of outward current was detectable in either high K^+ (90 mM) or low K^+ (30 mM) solutions (Figures 1A and 1B). Application of 3 μM carbachol (an agonist of m1 AChR) to these oocytes in the presence of 50 μM DIDS, a chloride channel blocker, caused a slow inhibition of the IRK3 K^+ channels (Figures 1D and 1E), which outlasted the transient activation of the residual endogenous outwardly rectifying Ca^{2+}-activated chloride channels (Figures 1C and 1D). The extent of IRK3 inhibition ranged from 20% to 70% with an average of 42.5% ± 3.1% (n = 25). After carbachol was washed out, the IRK3 current slowly recovered in 15–40 min (Figures 1D and 1E), even when we perfused the oocytes with a solution containing 5 μM atropine, a cholinergic antagonist that should abolish m1 AChR stimulation. Stronger and faster modulation was observed when m1 AChR was expressed at a high level (not shown). The carbachol-induced inhibition of IRK3 current was not observed in oocytes expressing IRK3 alone. Mb-IRK2 (Kir2.2) was also inhibited by m1 AChR, albeit to a lesser extent. By contrast, IRK1 (Kir2.1) was not sensitive to m1 modulation (Figures 1F and 1G).

m1 Inhibition of IRK3 Involves a Novel Diffusible Second Messenger

The IRK3 current recorded from a cell-attached membrane patch was inhibited when carbachol was applied to the bath outside the patch electrode (n = 4) (Figure 2A). The inhibition and recovery had a time course similar to that from whole oocyte recording (Figures 1F and 2A). Thus, a diffusible factor mediates the m1 modulation.

M1 receptor stimulation is known to activate $G_{q/11}$ and phospholipase C-β (PLC-β). The activated PLC-β hydrolyzes phosphatidyl-inositol-bis-phosphate (PIP_2) to produce IP_3 and DAG. The former releases Ca^{2+} from an internal store and the latter activates PKC (Peralta et al., 1988; Caulfield, 1993), which may increase tyrosine kinase activity (Huang et al., 1993; Lev et al., 1995). To

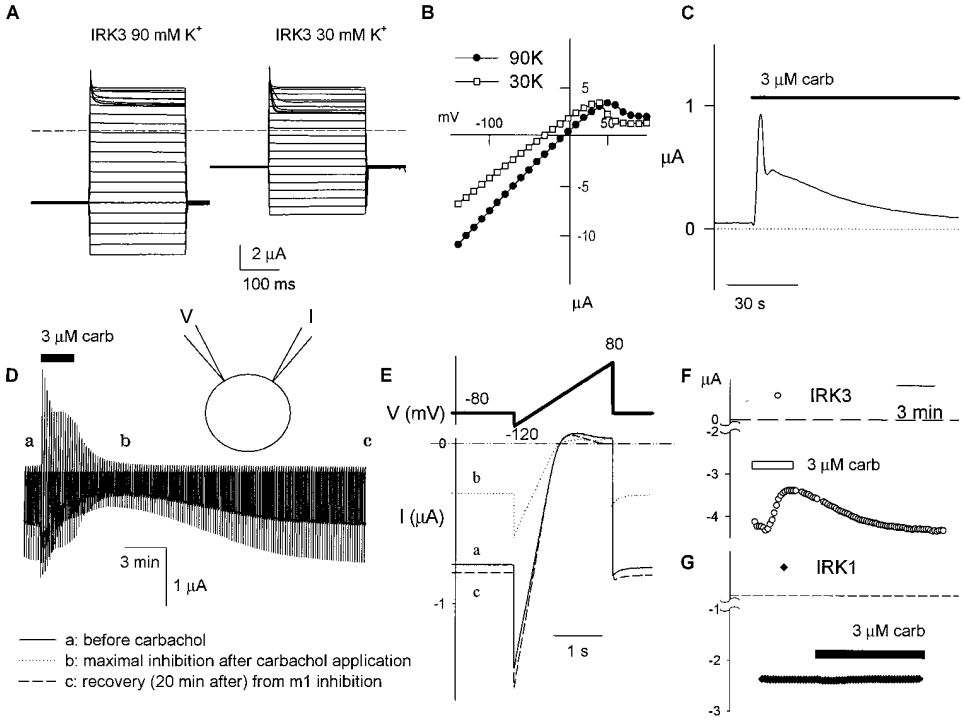

Figure 1. IRK3 Current Is Inhibited by m1 AChR Stimulation

(A) IRK3 currents from the same oocyte in bath solutions with 90 mM or 30 mM K^+. The membrane potential was held at −80 mV and subjected to 250 ms voltage steps ranging from +100 mV to −130 mV with 10 mV decrements.

(B) The current–voltage relationship of IRK3 in 90 mM K^+ (circles) and 30 mM K^+ (squares) solutions.

(C) A residual Ca^{2+}-activated Cl^- current (at +40 mV) was induced by m1 AChR stimulation by 3 μM carbachol in the presence of 50 μM DIDS. This outwardly rectifying chloride current had a small amplitude and decayed rapidly in 2–3 min, so that it did not interfere with the measurement of IRK3 inward current.

(D) m1 AChR stimulation caused slow inhibition of IRK3 currents. The Ca^{2+}-activated chloride current (see [1C]) gave rise to the upward deflections in this panel. The maximal inhibition (at the time point marked as [b]) occurred about 4 min since the start of carbachol application.

(E) Top, the voltage ramp protocol. Bottom, three ramp traces from the oocyte shown in (1D) were superimposed to demonstrate the reversible m1 modulation of IRK3. The small letters represent the time points in (D).

(F and G) The IRK3 current was reversibly inhibited by stimulation of m1 AChR, while the IRK1 current was not.

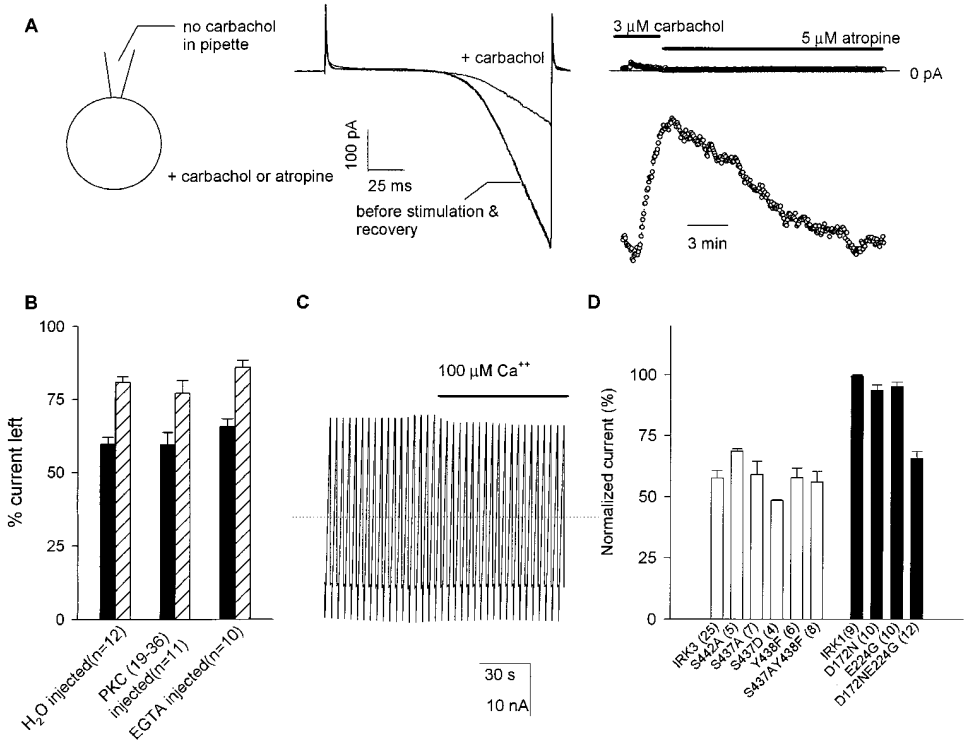

Figure 2. The m1 AChR Modulation Involves a Novel Diffusible Second Messenger

(A) M1 modulation of IRK3 is mediated by a cytoplasmic diffusible second messenger. (Left) Cartoon showing that bath application of carbachol modulates IRK3 in a cell-attached membrane patch. (Middle) IRK3 currents (before receptor stimulation, during maximal inhibition by m1AChR, and following recovery) from a cell-attached membrane patch subjected to a voltage ramp from +60 mV to −80 mV with 0 mV holding potential. (Right) The circles for the upper trace represent the scaled leak current at +80 mV. The time course of IRK3 modulation (inward current at −80 mV, lower trace) is similar to that recorded from whole oocyte (see Figure 1F).

(B) PKC inhibitor (50 nl, 2 mM stock) or EGTA (50 nl, 50 mM stock) injection did not preclude m1 AChR–mediated modulation of IRK3. The solid bars indicate the remaining IRK3 current (slope conductance at −110 mV normalized against the current before agonist application, in a bath solution with 80 mM K^+) at maximal inhibition within 5 min after application of 3 μM carbachol. The hatched bars show the normalized current 10 min after washing out carbachol. All oocytes included in this analysis were from the same batch and had leak current <400 nA at +80 mV. DIDS (50 μM) was added to all solutions to suppress the endogenous chloride currents except for the EGTA injection experiments.

(C) Application of 100 μM free Ca^{2+} to IRK3 channels in the inside-out patch led to a small increase in inward rectification but no change in the amplitude of inward current.

(D) Sensitivity of IRK3, IRK1, and their mutants to m1 modulation. The number of experiments is indicated in parentheses.

identify the second messenger that causes IRK3 channel inhibition, we began with several tests for the possible involvement of PKC. First, we examined the effects of phorbol ester, which activates PKC, and found that treatment of oocytes with 100 nM 4-β phorbol ester (PMA) inhibited IRK3 current irreversibly. However, the inactive isomer 4-α PMA, which does not activate PKC, also showed some inhibitory effect. We then injected oocytes with the peptide inhibitor of PKC, PKC 19–36. This treatment attenuated the m1 modulation of Kv1.2 channels (data not shown; see Huang et al., 1993) but not the m1 modulation of IRK3 channels (Figure 2B). Moreover, application of the catalytic subunits of PKC to inside-out patches did not alter IRK3 channel activity (n = 5, data not shown). It thus appears unlikely that PKC is essential for the IRK3 channel inhibition by m1 AChR.

Next, we tested for the possible involvement of Ca^{2+} by injecting EGTA into oocytes. This treatment prevented m1 AChR from inducing the Ca^{2+}-activated Cl^- current (data not shown), but did not abolish m1 modulation of IRK3 current (Figure 2B). Application of 5 μM A23187, a Ca^{2+} ionophore, for 15 min in a bath solution containing 2 mM Ca^{2+} increased the intracellular free Ca^{2+} level and induced the Ca^{2+}-activated chloride current, but it did not cause any reduction of IRK3 current (data not shown). Finally, application of 100 μM Ca^{2+} to IRK3 channels in inside-out membrane patches did not cause significant channel inhibition (Figure 2C). These studies indicate that Ca^{2+} does not mediate IRK3 channel inhibition by m1 AChR.

We also applied other second messenger candidates to IRK3 channels in inside-out membrane patches and found no significant channel inhibition by 10 μM IP_3 and/or 10 μM IP_4, up to 200 μM DAG (1-stearoyl-2-linoleoyl-sn-glycerol or 1-stearoyl-2-arachidonoyl-sn-glycerol), PLC (up to 2 U/ml), or PI-specific PLC (up to 0.5 U/ml). We have thus found no evidence implicating any of the known second messengers in the m1 receptor–mediated IRK3 channel inhibition.

The m1 Modulation of IRK3 Channels Cannot Be Accounted for by Channel Phosphorylation

Three lines of evidence indicate that m1 modulation of IRK3 channels is not due to channel phosphorylation.

Table 1. Inhibitory Effects of m1 AChR Stimulation on Wild-Type and Mutant IRK Channels

Chimeras generated between IRK3 and IRK1, listed in the first column, are depicted schematically in the last column (solid bars represent IRK3 sequences and open bars indicate IRK1 sequences). Potential phosphorylation sites for PKC or PKA (S36, S39, S348, S437, and S442) are marked with asterisks. Whether a chimera is (Y) or is not (N) sensitive to m1 modulation is indicated in the third column. A chimera is regarded as insensitive if there was <10% inhibition of current after applying 3 μM carbachol for 5 min. The percentage of inhibition (mean ± SEM) and the number of experiments are given in the second and the fourth columns.

construct	I_{min}/I_0(%)	modula-tion	n	fragment(s)transferred or deleted
IRK1	99.5 ± 0.5	N	9	
IRK3	57.5 ± 3.1	Y	25	
mb-IRK2	94.2 ± 3.5	N	5	
Chimeras				
K13-NMC	74.0 ± 0.8	Y	7	1-444
K13-N_0MC	74.6 ± 3.5	Y	8	14-444
K13-C_1	96.4 ± 0.8	N	27	222-444
K13-C_2	97.3 ± 1.1	N	6	272-444
K13-C_3	95.4 ± 2.5	N	5	342-444
K13-C_4	97.4 ± 0.9	N	8	425-444
K31-NMC_0	93.7 ± 1.2	N	8	1-221
K31-NM	96.2 ± 1.4	N	6	1-112
K31-N_1	96.0 ± 0.9	N	5	1-43
K31-N_2	98.5 ± 0.7	N	7	1-39
K31-N_3	98.6 ± 0.8	N	4	1-31
K313-N_1C_1	67.3 ± 4.2	Y	4	1-43, 222-444
K313-N_1C_4	97.8 ± 1.5	N	6	1-43, 425-444
K313-N_1C_3	97.8 ± 1.1	N	12	1-43, 342-444
K313-N_2C_1†	63.5 ± 6.7	Y	6	1-39, 222-444
K313-N_3C_1†	52.1 ± 7.1	Y	10	1-31, 222-444
K131-N_4	94.9 ± 3.1	N	4	14-31
K313-N_3C_2	71.2 ± 2.0	Y	6	1-31, 272-444
K1313-N_4C_2†	62.2 ± 3.9	Y	10	14-31, 272-444
K1313-N_5C_2†	76.4 ± 4.6	Y	12	14-27, 272-444
K13131-N_5C_5#	86.8 ± 2.7	Y	13	14-27,272-342**
K13131-N_5C_6	99.3 ± 1.2	N	7	14-27,272-281
Deletion mutants				
IRK3 VGAPΔ	60.2 ± 2.5	Y	4	90-110
IRK3 Pro5Δ	60.2 ± 9.9	Y	3	361-366
IRK3 ApaIΔ†	67.5 ± 5.6	Y	6	385-403

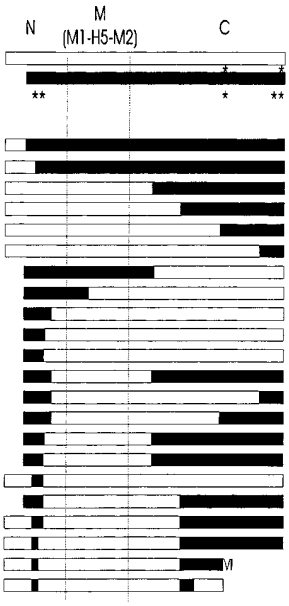

N_5 fragment sequence

```
IRK1   TRQQCRSRFVKKDGH
IRK3   RRKKRTRNRFVKKNGQ
```

C_5 fragment sequence

```
IRK1   DLSKQDIDNADFEIVVILEGMVEATAMTTQCRSSYLANEILWGHRYEPVLFEEKHYYKVDYSRFHKTYEVP
IRK3   GMGKEELESEDFEIVVILEGMVEATAMTTQARSSYLASEILWGHRFEPVVFEEKSHYKVDYSRFHKTYEVA
```

Sequence alignment of IRK1 and IRK3 in the N_5 and C_5 fragments is given under the table.

** K13131-N_5C_5 has two extra amino acid residues V and I at position 343 and 344.

† For some clones with lower expression levels, the bath solution contained 75 mM K^+.

First, IRK3 mutations of potential phosphorylation sites for PKC or tyrosine kinase did not abolish m1 modulation (Figure 2D). Second, no potential phosphorylation sites were created or removed by a double mutation that conferred sensitivity to m1 modulation to IRK1 (Figures 1G and 2D). Finally, a chimera that corresponds to a truncated IRK1 with 23 point mutations also acquired sensitivity to m1 modulation without acquiring any potential phosphorylation sites (see below).

Deletions of regions unique to IRK3, such as the VGAP region (aa 91–110) within the extracellular loop (Perier et al., 1994) and a proline-rich segment (aa 361–366) followed by multiple acidic residues (aa 385–403) in the C terminus, did not abolish m1 modulation (Table 1, deletion mutants, IRK3-VGAPΔ, IRK3-Pro5Δ, and IRK3-ApaIΔ). Chimeras were then made between IRK3 and IRK1 (Table 1). All these chimeras gave rise to strongly inwardly rectifying K^+ currents, with a voltage dependence that shifted with the potassium equilibrium potential (E_K) as external K^+ concentrations were varied, similar to the wild-type channels.

Neither the C terminus nor the N terminus of IRK3, when transplanted alone to IRK1, was sufficient to confer m1 modulation (Table 1, K13-C_1, K31-NMC_0, K31 NM, and K31-N_1). m1 modulation was restored only when both the C and N termini of IRK3 were grafted into IRK1 (Table 1, K313-N_1C_1). The smallest IRK3 segments that are sufficient to confer sensitivity to m1 modulation include 14 amino acids (aa 14–27, fragment N_5) in the N terminus and a conserved 71–aminoacid segment (aa 272–342, fragment C_5) in the C terminus (Table 1, K13131-N_5C_5). The N_5 fragment contains no serine, threonine, or tyrosine residues. Nine out of the 16 residues that are different between IRK3 and IRK1 in the C_5 fragment are included in the C_6 fragment of the chimera K13131-N_5C_6, which is insensitive to m1 modulation. The remaining seven amino acid substitutions in the C_5 fragment do not introduce any new phosphorylation sites. Thus, both hydrophilic domains of IRK3 contain sequences necessary for m1 modulation, which does not appear to be mediated by channel phosphorylation.

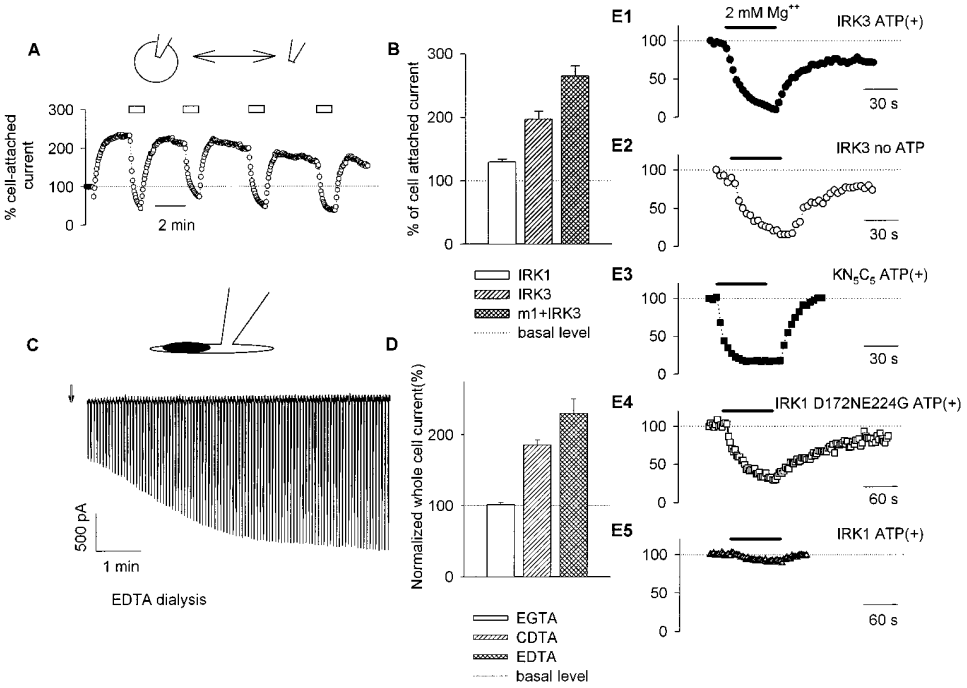

Figure 3. IRK3 Is Chronically Inhibited in Oocytes and Mammalian Cells in the Absence of m1 AChR Stimulation

(A) Excision of a membrane patch from an oocyte injected with *IRK3* cRNA alone causes IRK3 current to increase by about 100% (shown as the slope conductances between −60 and −50 mV normalized to those recorded from the cell-attached membrane patch). Cramming the patch deeply into the same oocyte (open boxes; see cartoon above) led to current inhibition.

(B) The current increases upon excision of the membrane patch from oocytes expressing IRK3 (n = 9), or IRK3 plus m1AChR (n = 15), but not IRK1 (n = 11). The bath contained 50 μM carbachol. Percent of cell-attached current is the largest conductance obtained following patch excision and before channel rundown, normalized against the conductance for the same membrane patch before excision, during cell-attached patch recording.

(C) Current from HEK 293 cell transfected with IRK3 slowly increased after the membrane under the patch electrode was broken off (arrow), presumably due to dialysis of the cytosol via the pipette solution during whole cell recording (see cartoon).

(D) The gradual increase of current was observed when the primary chelator in the pipette solution was EDTA (n = 11) or CDTA (n = 15), but not EGTA (n = 15). The "normalized whole cell current" is determined by measuring the slope conductance between −90 and −70 mV and normalizing it against that within the first minute of whole cell recording.

(E1–E5) Mg^{2+} inhibition of IRK3, and IRK1 chimera or mutant that acquired sensitivity to m1 modulation. Bars indicate application of Mg^{2+}. No correction for rundown was made.

Chronic Inhibition of IRK3 Channels in the Absence of m1 Receptor Stimulation

In experiments designed to examine the inhibitory effects of the diffusible factor for m1 modulation, we excised membrane patches from oocytes expressing IRK3 alone or together with m1 AChR (Figures 3A and 3B). Not only were IRK3 channels inhibited in oocytes that also expressed m1 AChR, but we also observed inhibition in oocytes expressing IRK3 alone. The extent of this chronic inhibition in the absence of m1 AChR stimulation was smaller than the extent of channel inhibition in oocytes that expressed IRK3 and the m1 AChR, and were stimulated with 50 μM carbachol (Figures 3A and 3B). Unlike IRK3, the IRK1 current showed little increase upon excision of the membrane patch from the oocyte (Figure 3B).

Given that IRK3 but not IRK1 channels are sensitive to m1 modulation as well as chronic inhibition by a cytoplasmic factor, we wondered whether the factor mediating chronic inhibition is also responsible for channel inhibition by m1 AChR. In this scenario, the inhibitory factor is present in the unstimulated oocyte and causes chronic inhibition; m1 receptor stimulation simply raises the concentration of the inhibitory factor and causes further suppression of current.

Chronic Inhibition of IRK3 Is Mediated by Intracellular Mg^{2+}

Chronic inhibition of IRK3 was also observed in CHO (Chinese hamster ovary) cells and HEK (human embryonic kidney) 293 cells transfected with IRK3. After a tight seal was formed between the patch electrode and a HEK 293 cell, the membrane patch was broken off to expose the cytosol to the pipette solution, and to allow current recording in the whole cell configuration. The gradual increase of IRK3 current revealed channel inhibition by a cytoplasmic factor that may be slowly lost into the pipette solution (Figure 3C). Inclusion of 10 mM ATP, 10 mM AMPPNP, 10 mM AMPPCP, or 2 mM ADP in the pipette solution did not prevent the IRK3 current from increasing during whole-cell recording, indicating that the chronic inhibition could not be due to channel inhibition by ATP. Inclusion of protein phosphatase inhibitors such as 1 μM okadaic acid, 10 mM orthovanadate, or

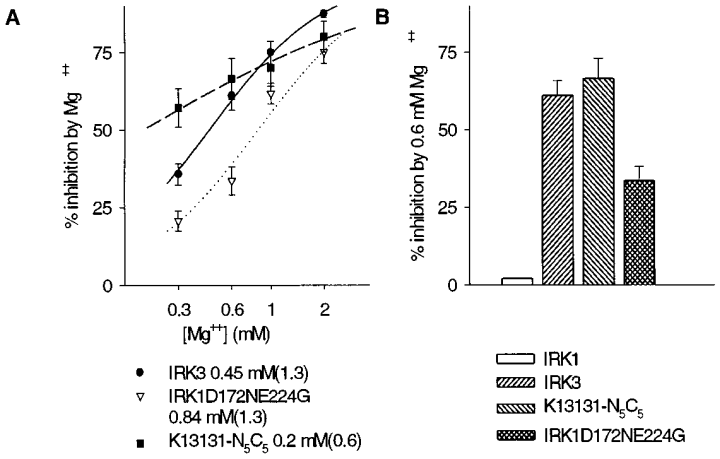

Figure 4. Quantitative Tests of the Magnesium Hypothesis

(A) Concentration dependence of Mg^{2+} inhibition of the three channel types that are sensitive to m1 modulation. Rundown of currents in excised patch was corrected by periodically switching the perfusion solution to a solution containing 10 mM EDTA and fitting the slow decrease (rundown) of current with a monoexponential function. The numbers beside the channels are the best-fit EC_{50} (n) for the equation: % inhibition = $100/\{1+(EC_{50}/[Mg^{2+}])^n\}$.

(B) Bar diagram showing that, unlike IRK1, all three K^+ channels that are sensitive to m1 modulation are also sensitive to inhibition by 0.6 mM Mg^{2+}.

(C1–C3) Tests for the hypothesis that Mg^{2+} mediates the m1 modulation.

(C1) Based on the dose–response curve in (A), we predicted the free Mg^{2+} concentrations of the batch of oocytes in Figure 3B, with and without m1 AChR stimulation.

(C2) Predicted extents of m1 modulation (see text) as compared with the observed values.

(C3) A similar test using another batch of oocytes. Pairs of Mg^{2+} concentrations that could give rise to the observed 42.5% inhibition of IRK3 whole cell current were taken from the dose–response curve of IRK3 and applied to the dose response curve of IRK1 D172NE224G to predict the extent of m1 inhibition (31.1% ± 6.9%) of this mutant channel. All numbers are expressed as mean ± SEM.

C1

m1 AChR stimulation	% inhibition of IRK3 channels (observed)	[Mg++]i (predicted)
-	50%	~ 0.5 mM
+	63%	~ 0.7 mM

C2

% whole cell current inhibited by m1 AChR stimulation

	predicted	observed
IRK3	28.3 ± 7.1 %	25.0 ± 2.4 %
K13131-N5C5	13.5 ± 7.6 %	13.2 ± 2.7 %

C3

% m1 inhibition on whole cell currents

	predicted	observed
IRK3	N/A	42.5 ± 3.1 %
IRK1 D172NE224G	31.1 ± 6.9 %	34.6 ± 3.1 %

40 μM genestein (a tyrosine kinase inhibitor) both in the bath and in the pipette solution also did not prevent the IRK3 current from increasing, suggesting that the chronic inhibition could not be accounted for by channel phosphorylation. A similar conclusion was also obtained for chronic inhibition in the oocyte when we applied these phosphatase inhibitors to IRK3 channels in inside-out membrane patches.

The increase of IRK3 current was observed when the cytosol came in contact with pipette solution containing either EDTA or CDTA, but not when the cytosol was exposed to pipette solution containing EGTA (Figure 3D). The major difference between EDTA and EGTA is the ability of the former but not the latter to chelate Mg^{2+}. This led us to investigate whether Mg^{2+} exerts any inhibitory effect on IRK3 channels as well as the IRK1 mutants that are sensitive to m1 modulation.

Mg^{2+} inhibited IRK3, K13131-N_5C_5, and IRK1 D172NE224G, but not IRK1 in inside-out patches from Xenopus oocytes (Figures 3E1-3E5). K13131-N_5C_5 was more sensitive to Mg^{2+} but had a relatively flat concentration dependence curve, whereas IRK3 and IRK1 D172NE224G had steeper dose–response curves (Figures 4A and 4B). By contrast, IRK1 was essentially not inhibited by up to 2 mM Mg^{2+} (Figures 3E5 and 4B). Mg^{2+} inhibition of both inward and outward current had a slow time course (Figures 6D and 6E) and was independent of membrane potential (Figure 6E). This inhibitory effect of Mg^{2+} is therefore clearly distinguishable from the rapid and voltage-dependent action of Mg^{2+} as a pore blocker (Figures 6D–6F) (Matsuda et al., 1987; Vandenberg, 1987; Ficker et al., 1994; Lopatin et al., 1994; Stanfield et al., 1994; Fakler et al., 1995; Yang et al., 1995).

A Long Inactivated State Accounts for the Chronic Inhibition of IRK3

Having found that IRK3 channels are chronically inhibited by Mg^{2+} inside the cell, we did single channel recording to determine the mechanism of this chronic inhibition. In the cell-attached configuration, the IRK3 channels tended to enter a prolonged inactivated state (lasting for 1–5 min for channels in which we observed subsequent openings). Usually two to three such long inactivating events took place within 10 min of continuous recording. Occasionally all the channels of a patch entered the long inactivated state, resulting in brief quiescence without any channel activity. Figure 5A is an

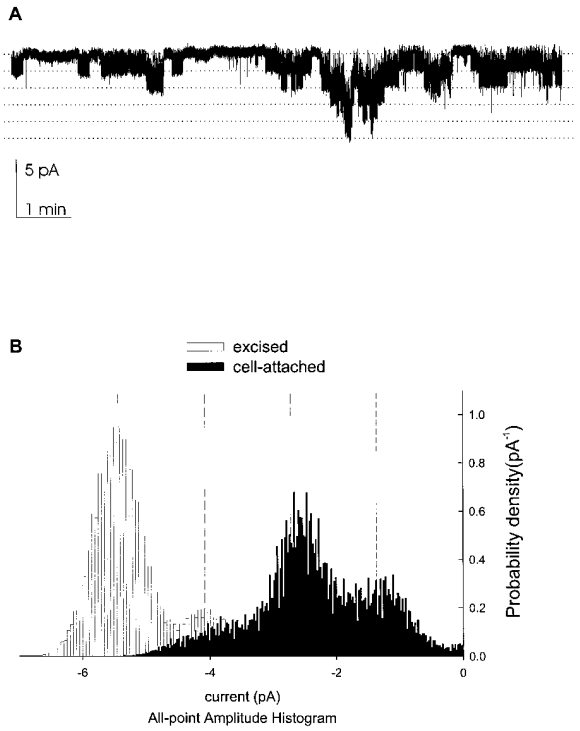

Figure 5. Chronic Inhibition of IRK3 Channels Is Due to Prolonged Channel Inactivation

(A) Chronic inhibition of IRK3 channels as revealed by continuous recording from a cell-attached patch of HEK 293 cell stably transfected with IRK3. The lines indicate the expected currents for 0–5 active channels. Most frequently we saw two channels active simultaneously.

(B) All-point amplitude histogram for a membrane patch from an oocyte expressing IRK3. During 30 min of cell-attached recording, we never observed all four channels being active simultaneously. Often only one or two channels were active. Excision of the patch into the bath with 10 mM EDTA and no Mg^{2+} revealed four active channels. (The amplitude histogram was compiled from recording 60 s to 300 s after patch excision, prior to channel rundown.) The probability density for the patch current amplitude is the fraction of time when that current amplitude is observed divided by the bin width (0.0244 pA for cell-attached recording and 0.0488 pA for excised patch recording). The relative frequencies P(n) for n active channels in the histogram (indicated by the vertical dashed lines) are: P(0)=0.028, P(1)=0.333, P(2)=0.445, and P(3)=0.194 at cell attached configuration; P(2)=0.002, P(3)=0.198, P(4)=0.800 after patch excision. For analysis and display, data were filtered at 0.5 kHz.

example of such a patch with at least five channels, though most often one or two of these channels were active. After the membrane patch was excised, the IRK3 channels did not enter the inactivated state so readily, leading to almost full channel activation. This is illustrated in the histogram in Figure 5B for recordings from an oocyte membrane patch containing at least four channels.

Like IRK3, the chimera K13131-N_5C_5 also entered a long inactivated state frequently. In contrast, IRK1 rarely entered a long inactivated state; the longest duration of inactivation from three different patches was less than 30 s. Thus, IRK3 but not IRK1 channels are susceptible to m1 modulation and chronic inhibition, which could be accounted for by the ability of Mg^{2+} to promote the long–lasting inactivation.

Susceptibility to m1 Modulation Correlates with the Sensitivity to Mg^{2+} Inhibition but Not the Sensitivity to Mg^{2+} Block of the Channel Pore

Close examination of IRK3 modulation by m1 AChR revealed that the outward current was reduced to a greater extent than the inward current (Figure 6A). Thus, m1 receptor stimulation not only reduced the current amplitude but also increased the extent of inward rectification, probably owing to a block of the channel pore by polyamines or Mg^{2+}. There is, however, rather poor correlation between the susceptibility to m1 AChR-mediated channel inhibition and the sensitivity to Mg^{2+} and polyamines as pore blockers (Yang et al., 1995; this study). In fact, K13131-N_5C_5 approached IRK1 in its strong susceptibility to pore block by polyamines (data not shown) and Mg^{2+} (Figure 6C), and yet it is sensitive to m1 modulation (Table 1) whereas IRK1 is not (Figure 6B).

By contrast, there is good correlation between m1 modulation and the voltage-independent Mg^{2+} inhibition: unlike IRK1, IRK3 and the two IRK1 mutants that have acquired sensitivity to m1 modulation are all subjected to chronic inhibition as well as Mg^{2+} inhibition (Figures 3–5). We therefore examined the hypothesis that m1 AChR stimulation causes an increase in free Mg^{2+} concentration and that Mg^{2+} inhibition underlies both chronic inhibition and m1 receptor–induced inhibition of inward rectifier K^+ channels.

Tests of the Mg^{2+} Hypothesis

First, we assumed that the observed chronic inhibition of IRK3 (Figure 3B) was due to Mg^{2+} inhibition and used the dose–response curve for Mg^{2+} inhibition of IRK3 current (Figure 4A) to predict the free Mg^{2+} concentration inside an oocyte ($\sim$0.5 mM) (Figure 4C1). We then applied this value to the Mg^{2+} dose–response curves for the two IRK1 mutants (Figure 4A) to predict the extent of their chronic inhibition. These predicted values approximated the measured levels of chronic inhibition (63% versus 62% for K13131-N_5C_5 and 28% versus 31% for IRK1 D172NE224G).

Second, if we assumed that the greater extent of IRK3 channel inhibition in oocytes with m1 AChR stimulation (Figure 3B) was also due to Mg^{2+} inhibition, we could estimate the free Mg^{2+} concentration to be about 0.7 mM in oocytes with m1 AChR stimulation (Figure 4C1). Based on the dose-response curves (Figure 4A), we could predict the extents of m1 inhibition and compare that with the current inhibition measured by a two-electrode voltage clamp. Again, the predicted current inhibition was close to the measurements (Figure 4C2). All of the oocytes used in the above two tests were from the same batch, because Mg^{2+} concentration variations among different batches of oocytes may arise from the differences in the physiological or metabolic state of the frog.

To test further the hypothesis that Mg^{2+} inhibition underlies m1 modulation, we used a two-electrode voltage clamp to measure the extent of m1 AChR-induced current inhibition for IRK3 and IRK1 D172NE224G expressed in another batch of oocytes. We relied on the

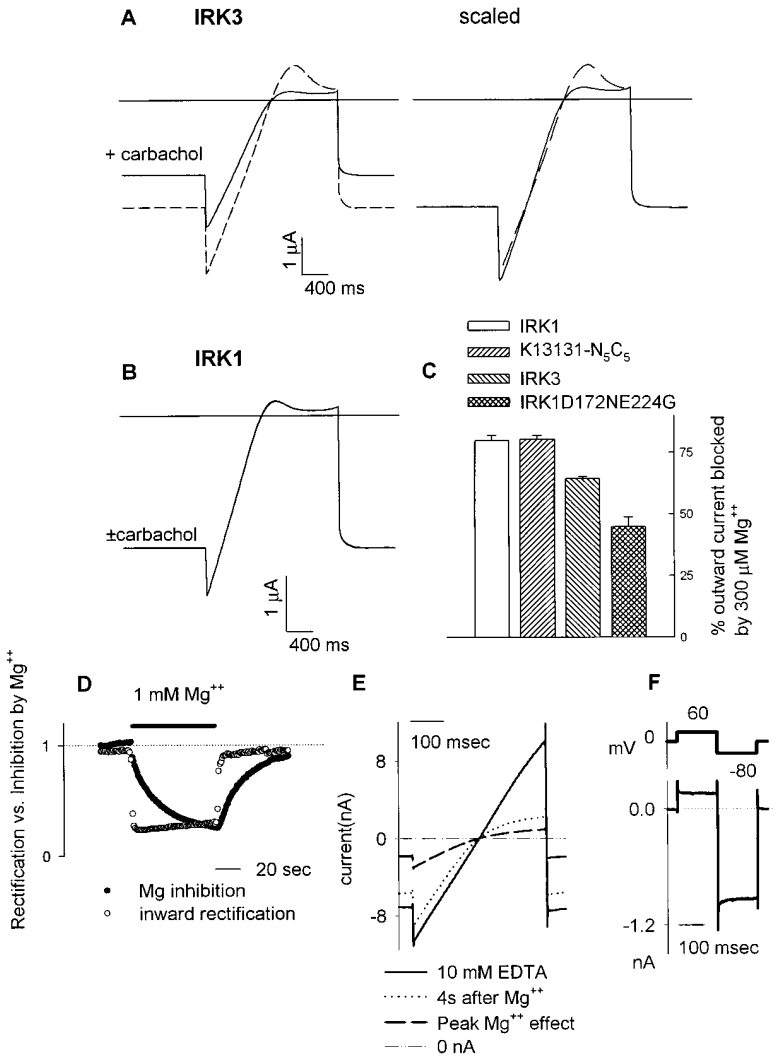

Figure 6. Susceptibility to m1 Modulation Does Not Correlate with Sensitivity to Mg^{2+} Block of the Channel Pore

(A) Left panel shows IRK3 currents at maximal inhibition (solid line) and recovery from m1 modulation (dashed line). Right: the current at −80 mV in the presence of carbachol (solid line) was scaled up to match the current after recovery (dashed line) to demonstrate an increase in inward rectification.

(B) IRK1 currents before and after m1 receptor stimulation were superimposable.

(C) Sensitivity to Mg^{2+} as a pore blocker: 300 μM Mg^{2+} blocked a larger fraction of the outward current of IRK1 and K13131-N_5C_5, as compared to IRK3 and IRK1 D172NE224G.

(D) Inward rectification caused by Mg^{2+} blocking the channel pore (open circles, the current at +60 mV divided by that at −60 mV) is immediate, whereas the inhibitory effect of Mg^{2+} (closed circles, shown as the inward current at −40 mV normalized against that in the absence of Mg^{2+}) takes about 1 min to reach maximal effect.

(E) The inhibition of IRK3 by Mg^{2+} is voltage-independent (peak Mg^{2+} effect), while the pore-blocking effect of Mg^{2+} is voltage-dependent (4 s after Mg^{2+}).

(F) Top, the pulse protocol. Bottom, in 1 mM free Mg^{2+}, the voltage-dependent block and unblock were almost instantaneous.

fact that the dose–response curves for Mg^{2+} inhibition of these two channel types are roughly parallel (Figure 4A), and used the measured inhibition of IRK3 current to predict the extent of inhibition of IRK1 D172NE224G (Figure 4C3). Once again, the agreement between the predicted and observed inhibition supports the idea that Mg^{2+} is the messenger for m1 modulation of these channels.

Discussion

We have found that a novel second messenger is responsible for m1 AChR–mediated inhibition of inward rectifier K^+ channels expressed in the Xenopus oocytes. As discussed below, a strong candidate for this novel second messenger is the Mg^{2+} ion.

A Novel Second Messenger for m1 Modulation of IRK3

The m1 AChR–mediated channel inhibition is due to a cytoplasmic diffusible second messenger (Figure 2A). PKC and channel phosphorylation cannot account for m1 modulation for the following reasons. First, the m1 modulation was not blocked by injecting PKC 19–36 into the oocyte (Figure 2B). Second, mutations of IRK3 eliminating potential PKC phosphorylation sites did not abolish m1 modulation. Third, of the two IRK3 fragments conferring the minichimera K13131-N_5C_5 with the susceptibility to m1 modulation, no residues in the N_5 region could be phosphorylated, and the C_5 region, which is 80% identical to its counterpart in IRK1, does not contain additional potential PKC phosphorylation sites. Fourth, the double mutation D172NE224G of IRK1 rendered the mutant channel sensitive to m1 inhibition without creating any sites for PKC phosphorylation. Finally, direct application of PKC to the cytoplasmic side of excised membrane patches did not inhibit IRK3 channel activities. It thus appears that m1 inhibition of IRK3 channel activity cannot be attributed to phosphorylation of IRK3 channels by PKC.

Other second messengers of the $G_{q/11}$ pathway include PLC, IP_3, IP_4, DAG, and Ca^{2+}. Direct application of these potential second messengers to inside out patches had no inhibitory effect on IRK3 channels; neither did the use of Ca^{2+} ionophore A23187, which elevated the intracellular free Ca^{2+} concentration. Injecting the oocyte

with EGTA to chelate Ca^{2+} also failed to eliminate the m1 modulation. Taken together, these results suggest that m1 modulation of IRK3 channels involves a novel second messenger.

Mg^{2+} as a Physiological Messenger for IRK3 Modulation

In the absence of m1 AChR stimulation, about half of the IRK3 channels are inhibited in both Xenopus oocytes and mammalian cells. This chronic inhibition was relieved by EDTA and CDTA but not EGTA (Figures 3C and 3D), implicating cytoplasmic Mg^{2+} as the inhibitory factor. Indeed, IRK3 channels were inhibited by Mg^{2+} even in the absence of ATP, indicating that channel inhibition is likely due to free Mg^{2+} ions (Figure 3E). Half inhibition was achieved at ~0.5 mM Mg^{2+}, consistent with the idea that the physiological concentration (ranging from 0.2 to 2 mM) (Gupta et al., 1984) of Mg^{2+} can account for the chronic inhibition of IRK3 channels (Figures 4 and 5). Further evidence for Mg^{2+}-mediated chronic inhibition derives from the comparison of the extents of chronic inhibition observed for K13131-N_5C_5 (~63%) and IRK1 D172NE224G (~28%) with the predicted chronic inhibition based on their dose– response curves for Mg^{2+} inhibition and an assumed Mg^{2+} concentration of 0.5 mM (~62% for K13131-N_5C_5 and ~31% for IRK1 D172NE224G). In addition to IRK3, other ion channels and enzymes have been found to be regulated by free Mg^{2+} in the physiologically relevant concentration range (Cech et al., 1980; White and Hartzell, 1988, 1989; Hartzell and White, 1989; Agus and Morad, 1991; Rijkers and Griffioen, 1993).

Is it possible that Mg^{2+} also mediates m1 inhibition of IRK3 channels? Several observations agree with this hypothesis. First, the susceptibility of IRK3 but not IRK1 to m1 inhibition is paralleled by chronic inhibition and Mg^{2+} inhibition of the former but not the latter (Figures 1F, 1G, 3B, 3E, and 4B). Second, mutations of IRK1 that bestow the channels with the ability to respond to m1 modulation also confer sensitivity to Mg^{2+} inhibition (Figures 3 and 4). By assuming that Mg^{2+} is responsible for both chronic inhibition and m1 modulation (Figure 3B), we have estimated the Mg^{2+} concentration to be ~0.5 mM at rest and ~0.7 mM following m1 AChR stimulation (Figure 4C1). We have also attempted to use the fluorescent dye mag-fura-2 to detect changes of Mg^{2+} concentration due to carbachol stimulation in several mammalian cell lines that express m1 AChR. Given the relatively low sensitivity and poor specificity of this dye (K_d for Mg^{2+}: 1.5 mM; K_d for Ca^{2+}: 17 μM), it is not surprising that we failed to detect any reliable signals in our imaging experiment, even though free Ca^{2+} rise could be detected using fura-2 imaging. Using the predicted Mg^{2+} concentrations (Figure 4C1), however, we could predict the extents of m1 inhibition of IRK3 and K13131-N_5C_5 (Figure 4C2) based on the dose–response curves for their inhibition by Mg^{2+} (Figure 4A). Another quantitative test (Figure 4C3) provides further support for the hypothesis that Mg^{2+} is the messenger that mediates channel inhibition by m1 AChR. Although we cannot exclude the possibility that an as-yet-unidentified messenger is the authentic mediator of m1 modulation, nor can we discount the possibility that m1 AChR activation can lead to some channel modification that changes the sensitivity of these channels to the Mg^{2+} inhibition, it seems quite likely that m1 AChR stimulation increases free Mg^{2+} concentration and causes channel inhibition because this scenario can quantitatively account for the differential sensitivities of IRK3, IRK1D172NE224G, and K13131-N_5C_5 channels to m1 modulation.

Mg^{2+} as a Candidate Mediator of m1 AChR Action

Mg^{2+} is the third most abundant cytoplasmic cation. Free Mg^{2+} represents only 2%–3% of the total cellular Mg^{2+} because the majority is sequestered in internal organelles, bound by cytosolic proteins, or complexed with small organic molecules such as nucleotides and metabolic intermediates including citric acid. Epinephrine and phorbol ester have been found to regulate Mg^{2+} influx and hence alter free Mg^{2+} level (Elliott and Rizack, 1974; Erdos and Maguire, 1983; Grubbs and Maguire, 1986). This mechanism cannot explain the m1 AChR-mediated inhibition of the IRK3 channel, because the inhibition persisted in the absence of external Mg^{2+}. Just how m1 AChR stimulation might lead to an increase of intracellular Mg^{2+} concentration is not known, but it could conceivably involve enzyme activities and/or Ca^{2+} mobilization. Indeed, the buffering capacity for Mg^{2+} may be altered by changes in metabolic state or signaling processes, such as local release of Ca^{2+} from the internal stores or transient change of intracellular pH, thereby altering the free Mg^{2+} concentration either globally or locally (Flatman, 1991; Murphy et al., 1991). Thus, free Mg^{2+} can potentially integrate the signals from hormone, cellular metabolism, organismal ion homeostasis and affect the activities of ion channels and other effectors.

Mg^{2+} Regulates IRK3 Channels via a Mechanism Different from Pore Block

What is the mechanism that allows Mg^{2+} to inhibit IRK3 channels in the absence of ATP? The inhibitory action of Mg^{2+} that underlies the chronic inhibition and possibly the m1 modulation of IRK3 channels differs from the known pore-blocking effect of Mg^{2+} for inward rectification (Matsuda et al., 1987; Vandenberg, 1987). The on and off rates for Mg^{2+} to block the pore and to reduce primarily the outward currents are fast (within milliseconds), whereas the inhibition of both inward and outward currents by Mg^{2+} is much slower in onset and recovery (almost 1 min) (Figures 6D and 6F). The concentration of free Mg^{2+} required for inward rectification gating is at least 10-fold lower than that for channel inhibition. The voltage dependence of these two effects also differs: whereas the pore-blocking effect is voltage-dependent (Figure 6F), the inhibitory action is almost insensitive to membrane potential (Figure 6E). This voltage-independent inhibition allows Mg^{2+} to affect channel activity near resting potential. Mg^{2+} inhibition probably arises from the channel entering a prolonged inactivated state and involves the two small regions of IRK3 that can transfer Mg^{2+} inhibition, chronic inhibition, and m1 modulation to the chimera K13131-N_5C_5. It will be of interest to determine whether Mg^{2+} stabilizes the long inactivated state by binding to the channel or to other

membrane-associated molecules that control channel gating.

Physiological Relevance of a Slow Modulation

The inward rectifier K^+ channels are active near the resting membrane potential and contribute to the membrane input resistance. The m1 AChR-mediated inhibition of IRK3 channel activities persists for a few minutes after receptor stimulation and is much slower than the activation of the G protein–gated inward rectifier K^+ channels by m2 AChR (in the range of milliseconds to seconds). The former allows the fine tuning of membrane resistance on a minute-to-minute or even slower basis, while the latter is suitable for rapid regulation of events such as heart beat. For tonic neurons in the sympathetic ganglia and many central neurons, fast synaptic inputs produce only small, subthreshold EPSPs that have to summate in order to fire an action potential (Crowcroft et al., 1971; McLachlan and Meckler, 1989). Integration of synaptic inputs may be more effectively regulated by a slow but persistent inhibition of inward rectifier K^+ channels as observed in this study.

Experimental Procedures

Electrophysiology

Stage V-VI oocytes were prepared from X. laevis (Goldin, 1992). In vitro–transcribed cRNAs (by Ambion or Epicenter Technology transcription kits) of IRK3 (2.5 ng) and/or m1AChR (25 ng) were injected into oocytes. Two- electrode voltage clamp recordings were performed 1–3 days after injection. Patch clamp recordings were done on days 5–14. The standard bath solution for most two-electrode voltage clamp experiments contained 60 mM Tris/Tris-HCl, 30 mM KCl, 2 mM $CaCl_2$, and 50 μM 4,4′-diisothiocyanatostilbene-2,2′-disulfonic acid (DIDS) (pH 7.4). To enhance the inward current amplitude, we sometimes replaced Tris/Tris-HCl with KCl. The standard pulse protocol for two-electrode voltage clamp experiments is shown in Figure 1E. For patch-clamp experiments, we adopted the giant patch technique (Collins et al., 1992) and used pipettes with tip diameters 30 to 60 μm. Data were sampled at 10 kHz and filtered at 5 kHz. The standard pulse protocol for giant patch recording was holding the membrane at −40 mV and giving a 400 ms ramp from −60 to +60 mV every 4 s. For continuous recording, the membrane was held at −100 mV, and currents were sampled at 10 kHz and filtered at 3kHz. The pipette solution for cell attached patch clamp experiments contained 5 mM HEPES, 145 mM KCl, 1 mM $MgCl_2$, and 1 mM $CaCl_2$ (pH 7.4) with or without 100 μM DIDS. In the experiment shown in Figure 2C, all Cl^- ions in the pipette solution were replaced with gluconate. For whole cell recording, the pipette solution contained 20 mM HEPES, 22 mM KOH, 20 mM KCl, 40 mM K_2SO_4, and 10 mM K_2-chelator (EGTA, CDTA, or EDTA) (pH 7.2). The standard bath solution for oocyte patch-clamp experiments contained 10 mM HEPES, 10 mM K_2EDTA, 20 mM KOH, 105 mM KCl, 5 mM KH_2PO_4, and 0.5 mM KF. Modifications are listed as follows. In Figure 2C, the Cl^- ions were replaced with gluconate. In Figure 3A, all anions were Cl^-. In Figure 3E, the perfusion solution contained 10 mM HEPES, 5 mM K_2EGTA, 5 mM KOH, 135 mM KCl, and varying amounts of Na_2ATP, $MgCl_2$, NaCl, and NaOH to achieve 4 mM MgATP, different Mg^{2+} concentrations calculated by Bound and Determined (Storey, 1992), at pH 7.2. The Na^+ concentration differences among these solutions were less than 5 mM. For Figure 3E2, EGTA replaced EDTA in the standard solution. For whole cell recording of the HEK 293 cells, the bath solution contained 130 mM Tris/Tris-HCl, 30 mM KCl, 1.8 mM $CaCl_2$, 0.8 mM $MgCl_2$, and 10 mM glucose (pH 7.4). The Tris/Tris-HCl was replaced with KCl to achieve 150 mM K^+ for cell-attached recordings. Pipettes for whole cell recording had 1.0–1.5 MΩ resistance when filled with the pipette solution. Capacitance cancellation and series resistance compensation were completed within 40 s of breaking into cells; otherwise the recording was discontinued. Only the cells having series resistance less than 4 MΩ, with more than 80% compensation and no deterioration of gigaohm seals, were used in the study of chronic inhibition. The voltage protocol was to hold the cell at 0 mV, followed by three consecutive 10 ms voltage steps to +10, +20, and -80 mV, and then an 80 ms ramp from -100 to +60 mV every 4 s.

Mammalian Cell Culture and Transfection

All mammalian cells were cultured with DMEM/F12 supplemented with 2 mM glutamine, 10% fetal bovine serum, and antibiotics at 37°C and 5% CO_2. HEK 293 cells were transfected with plasmid (pCDNA3, Invitrogen) encoding IRK3 cDNA using lipofectamine (GIBCO–BRL), selected in 0.7 mg/ml G418, and cloned according to the principle of limited dilution. A clonal cell line was used for this study.

Acknowledgments

The human m1 AChR cDNA was a kind gift of Dr. Bruce Conklin; IRK1 mutants were kindly provided by Dr. Jian Yang. Dr. Biao Zhao helped with the construction of chimeras K31-N_1, K31-NM, and K31-NMC_0. We also thank our colleagues for discussion and preparation of an earlier version of this manuscript. Y. N. J. and L. Y. J. are Howard Hughes Investigators. H.-h. C. is supported by the Biomedical Sciences Program at UCSF. This work is supported by an NIMH grant to the Silvio Conte Center of Neuroscience at UCSF.

Received December 6, 1996; revised May 12, 1997.

References

Agus, Z.S., and Morad, M. (1991). Modulation of cardiac ion channels by magnesium. Annu. Rev. Physiol. *53*, 299–307.

Braun, A.P., Fedida, D., and Giles, W.R. (1992). Activation of α1-adrenoceptors modulates the inwardly rectifying potassium currents of mammalian atrial myocytes. Pflügers Arch. *421*, 431–439.

Caulfield, M.P. (1993). Muscarinic receptors—characterization, coupling and function. Pharmacol. Ther. *58*, 319–379.

Caulfield, M.P., Jones, S., Vallis, Y., Buckley, N.J., Kim, G.D., Milligan, G., and Brown, D.A. (1994). Muscarinic M-current inhibition via $G\alpha_{q/11}$ and α-adrenoceptor inhibition of Ca^{2+} current via $G\alpha_o$ in rat sympathetic neurones. J. Physiol. *477*, 415–422.

Cech, S.Y., Broaddus, W.C., and Maguire, M.E. (1980). Adenylate cyclase: the role of magnesium and other divalent cations. Mol. Cell. Biochem. *33*, 67–92.

Collins, A., Somlyo, A.V., and Hilgemann, D.W. (1992). The giant cardiac membrane patch method: stimulation of outward Na^+-Ca^{2+} exchange current by MgATP. J. Physiol. *454*, 27–57.

Collins, A., German, M.S., Jan, Y.N., Jan, L.Y., and Zhao, B. (1996). A strongly inwardly rectifying K^+ channel that is sensitive to ATP. J. Neurosci. *16*, 1–9.

Crowcroft, P.J., Holman, M.E., and Szurszewski, J.H. (1971). Excitatory input from the distal colon to the inferior mesenteric ganglion in the guinea pig. J. Physiol. *219*, 443–461.

DiFrancesco, D., Noma, A., and Trautwein, W. (1980). Separation of current induced by potassium accumulation from acetylcholine-induced relaxation current in the rabbit S-A node. Pflügers Arch. *387*, 83–90.

Dukes, I.D., and Philipson, L.H. (1996). K^+ channels: generating excitement in pancreatic beta-cells. Diabetes *45*, 845–853.

Egan, T.M., and North, R.A. (1986). Acetylcholine hyperpolarizes central neurones by acting on an M_2 muscarinic receptor. Nature *319*, 405–407.

Elliott, D.A., and Rizack, M.A. (1974). Epinephrine and adrenocorticotropic hormone-stimulated magnesium accumulation in adipocytes and their plasma membranes. J. Biol. Chem. *249*, 3985–3900.

Erdos, J.J., and Maguire, M.E. (1983). Hormone-sensitive magnesium transport in murine S49 lymphoma cells: characterization and specificity for magnesium. J. Physiol. *337*, 351–371.

Fakler, B., Brandle, U., Glowatzki, E., Weidemann, S., Zenner, H.P., and Ruppersberg, J.P. (1995). Strong voltage-dependent inward rectification of inward rectifier K^+ channels is caused by intracellular spermine. Cell *80*, 149–154.

Ficker, E., Taglialatela, M., Wible, B.A., Henley, C.M., and Brown, A.M. (1994). Spermine and spermidine as gating molecules for inward rectifier K^+ channels. Science *266*, 1068–1072.

Flatman, P.W. (1991). Mechanisms of magnesium transport. Annu. Rev. Physiol. *53*, 259–271.

Goldin, A.L. (1992). Maintenance of Xenopus laevis and oocyte injection. Meth. Enzymol. *207*, 266–279.

Grubbs, R.D., and Maguire, M.E. (1986). Regulation of magnesium but not calcium transport by phorbol ester. J. Biol. Chem. *261*, 12550–12554.

Gupta, R.K., Gupta, P., and Moore, R.D. (1984). NMR studies of intracellular metal ions in intact cells and tissues. Annu. Rev. Biophys. Bioeng. *13*, 221–246.

Hartzell, H.C., and White, R.E. (1989). Effects of magnesium on inactivation of the voltage-gated calcium current in cardiac myocytes. J. Gen. Physiol. *94*, 745–767.

Hille, B. (1992). Ionic Channels of Excitable Membranes, Second Ed. (Sunderland, Massachusetts: Sinauer).

Huang, X.Y., Morielli, A.D., and Peralta, E.G. (1993). Tyrosine kinase-dependent suppression of a potassium channel by the G protein-coupled m1 muscarinic acetylcholine receptor. Cell *75*, 1145–1156.

Huang, C.-L., Slesinger, P.A., Casey, P.J., Jan, Y.N.,and Jan, L.Y. (1995). Evidence that direct binding of $G_{\beta\gamma}$ to the GIRK1 G protein-gated inwardly rectifying K^+ channel is important for channel activation. Neuron *15*, 1133–1143.

Inoue, M., Nakajima, S., and Nakajima, Y. (1988). Somatostatin induces an inward rectification in rat locus coeruleus neurones through a pertussis toxin-sensitive mechanism. J. Physiol. *407*, 177–198.

Jones, S., Brown, D.A., Milligan, G., Willer, E., Buckley, N.J., and Caulfield, M.P. (1995). Bradykinin excites rat sympathetic neurons by inhibition of M current through a mechanism involving B_2 receptors and $G\alpha_{q/11}$. Neuron *14*, 399–405.

Kofuji, P., Davidson, N., and Lester, H.A. (1995). Evidence that neuronal G-protein-gated inwardly rectifying K^+ channels are activated by G_γ subunits and function as heteromultimers. Proc. Natl. Acad. Sci. USA *92*, 6542–6546.

Krapivinsky, G., Krapivinsky, L., Wickman, K., and Clapham, D.E. (1995). $G_{\beta\gamma}$ binds directly to the G-protein-gated K^+ channel, I_{KACh}. J. Biol. Chem. *270*, 29059–29062.

Kunkel, M.T., and Peralta, E.G. (1995). Identification of domains conferring G-protein regulation on inward rectifier potassium channels. Cell *83*, 443–449.

Kurachi, Y., Nakajima, T., and Sugimoto, T. (1986). On the mechanism of activation of muscarinic K^+ channels by adenosine in isolated atrial cells: involvement of GTP-binding proteins. Pflügers Arch. *407*, 264–274.

Lev, S., Moreno, H., Martinez, R., Canoll, P., Peles, E., Musacchio, J.M., Plowman, G.D., Rudy, B., and Schlessinger, J. (1995). Protein tyrosine kinase PYK2 involved in Ca^{2+}-induced regulation of ion channel and MAP kinase functions. Nature *376*, 737–745.

Lopatin, A.N., Makhina, E.N., and Nichols, C.G. (1994). Potassium channel block by cytoplasmic polyamines as the mechanism of intrinsic rectification. Nature *372*, 366–369.

Marrion, N.V. (1996). Calcineurin regulates M channel modal gating in sympathetic neurons. Neuron *16*, 163–173.

Matsuda, H., Saigusa, A., and Irisawa, H. (1987). Ohmic conductance through the inwardly rectifying K channel and blocking by internal magnesium. Nature *325*, 156–159.

McLachlan, E.M., and Meckler, R.L. (1989). Characteristic of the synaptic input to three classes of sympathetic neurone in the coeliac ganglion of the guinea-pig. J. Physiol. *415*, 109–129.

Morishige, K., Takahashi, N., Jahangir, A., Yamada, M., Koyama, H., Zanelli, J.S., and Kurachi, Y. (1994). Molecular cloning and functional expression of a novel brain-specific inward rectifier potassium channel. FEBS Lett. *346*, 251–256.

Murphy, E., Freudenrich, C.C., and Lieberman, M. (1991). Cellular magnesium and Na/Mg exchange in heart cells. Annu. Rev. Physiol. *53*, 273–287.

Nakajima, Y., Nakajima, S., and Inoue, M. (1988). Pertussis toxin-insensitive G protein mediates substance P-induced inhibition of potassium channels in brain neurons. Proc. Natl. Acad. Sci. USA *85*, 3643–3647.

Noble, D. (1984). The surprising heart: a review of recent progress in cardiac electrophysiology. J. Physiol. *353*, 1–50.

North, R.A., and Uchimura, N. (1989). 5-Hydroxytryptamine acts at $5\text{-}HT_2$ receptors to decrease potassium conductance in rat nucleus accumbens neurones. J. Physiol. *417*, 1–12.

North, R.A., Williams, J.T., Surprenant, A., and Christie, M.J. (1987). μ and δ receptors belong to a family of receptors that are coupled to potassium channels. Proc. Natl. Acad. Sci. USA *84*, 5487–5491.

Oh, U., Ho, Y.K., and Kim, D. (1995). Modulation of the serotonin-activated K^+ channel by G protein subunits and nucleotides in rat hippocampal neurons. J. Membr. Biol. *147*, 241–253.

Peralta, E.G., Ashkenazi, A., Winslow, J.W., Ramachandran, J., and Capon, D.J. (1988). Differential regulation of PI hydrolysis and adenylyl cyclase by muscarinic receptor subtypes. Nature *334*, 434–437.

Perier, F., Radeke, C.M., and Vandenberg, C.A. (1994). Primary structure and characterization of a small-conductance inwardly rectifying potassium channel from human hippocampus. Proc. Natl. Acad. Sci. USA *91*, 6240–6244.

Rane, S.G., Walsh, M.P., McDonald, J.R., and Dunlap, K. (1989). Specific inhibitors of protein kinase C block transmitter-induced modulation of sensory neuron calcium current. Neuron *3*, 239–245.

Reuveny, E., Slesinger, P.A., Inglese, J., Morales, J.M., Iniguez-Lluhi, J.A., Lefkowitz, R.J., Bourne, H.R., Jan, Y.N., and Jan, L.Y. (1994). Activation of the cloned muscarinic potassium channel by G protein $\beta\gamma$ subunits. Nature *370*, 143–146.

Rijkers, G.T., and Griffioen, A.W. (1993). Changes in free cytoplasmic magnesium following activation of human lymphocytes. Biochem. J. *289*, 373–377.

Robbins, J., Marsh, S.J., and Brown, D.A. (1993). On the mechanism of M-current inhibition by muscarinic m1 receptors in DNA-transfected rodent neuroblastoma $\times$ glioma cells. J. Physiol. *469*, 153–178.

Sakmann, B., Noma, A., and Trautwein, W. (1983). Acetylcholine activation of single muscarinic K^+ channels in isolated pacemaker cells of the mammalian heart. Nature *303*, 250–253.

Sato, R., and Koumi, S. (1995). Modulation of the inwardly rectifying K^+ channel in isolated human atrial myocytes by α1-adrenergic stimulation. J. Membr. Biol. *148*, 185–191.

Selyanko, A.A., and Brown, D.A. (1996). Intracellular calcium directly inhibits potassium M channels in excised membrane patches from rat sympathetic neurons. Neuron *16*, 151–162.

Shen, K.Z., and North, R.A. (1992). Muscarine increases cation conductance and decreases potassium conductance in rat locus coeruleus neurones. J. Physiol. *455*, 471–485.

Sodickson, D.L. and Bean, B.P. (1996). GABAB receptor-activated inwardly rectifying potassium current in dissociated hippocampal CA3 neurons. J. Neurosci. *16*, 6374–6385.

Soejima, M., and Noma, A. (1984). Mode of regulation of the ACh-sensitive K-channel by the muscarinic receptor in rabbit atrial cells. Pflügers Arch. *400*, 424–431.

Stanfield, P.R., Nakajima, Y., and Yamaguchi, K. (1985). Substance P raises neuronal membrane excitability by reducing inward rectification. Nature *315*, 498–501.

Stanfield, P.R., Davies, N.W., Shelton, P.A., Khan, I.A., Brammar, W.J., Standen, N.B., and Conley, E.C. (1994a). The intrinsic gating of inward rectifier K^+ channels expressed from the murine IRK1 gene depends on voltage, K^+ and Mg^{2+}. J. Physiol. *475*, 1–7.

Stanfield, P.R., Davies, N.W., Shelton, P.A., Sutcliffe, M.J., Khan, I.A., Brammar, W.J., and Conley, E.C. (1994b). A single aspartate residue is involved in both intrinsic gating and blockage by Mg^{2+} of the inward rectifier, IRK1. J. Physiol. (Lond) *478*, 1–6.

Storey, K.B. (1992). Bound and determined: a computer program

for making buffer of defined ion concentrations. Anal. Biochem. *201*, 119–126.

Takano, K., Stanfield, P.R., Nakajima, S., and Nakajima, Y. (1995). Protein kinase C-mediated inhibition of an inward rectifier potassium channel by substance P in nucleus basalis neurons. Neuron *14*, 999–1008.

Uchimura, N., and North, R.N. (1990). Muscarine reduces inwardly rectifying potassium conductances in rat nucleus accumbens neurones. J. Physiol. *422*, 369–380.

Vandenberg, C.A. (1987). Inward rectification of a potassium channel in cardiac ventricular cells depends on internal magnesium ions. Proc. Natl. Acad. Sci. USA *84*, 2560–2564.

Velimirovic, B.M., Koyano, K., Nakajima, S., and Nakajima, Y. (1995). Opposing mechanisms of regulation of a G-protein-coupled inward rectifier K^+ channel in rat brain neurons. Proc. Natl. Acad. Sci. USA *92*, 1590–1594.

Wang, H.-S., and McKinnon, D. (1996). Modulation of inwardly rectifying currents in rat sympathetic neurones by muscarinic receptors. J. Physiol. *492*, 467–478.

White, R.E., and Hartzell, H.C. (1988). Effects of intracellular free magnesium on calcium current in isolated cardiac myocytes. Science *239*, 778–780.

White, R.E., and Hartzell, H.C. (1989). Magnesium ions in cardiac function. Regulator of ion channels and second messengers. Biochem. Pharmacol. *38*, 859–867.

Wickman, K.D., Iniguez-Lluhl, J.A., Davenport, P.A., Taussig, R., Krapivinsky, G.B., Linder, M.E., Gilman, A.G., and Clapham, D.E. (1994). Recombinant G-protein $\beta\gamma$-subunits activate the muscarinic-gated atrial potassium channel. Nature *368*, 255–257.

Yamada, M., Ho, Y.K., Lee, R.H., Kontanill, K., and Takahashill, K. (1994). Muscarinic K^+ channels are activated by $\beta\gamma$ subunits and inhibited by the GDP-bound form of a subunit of transducin. Biochem. Biophys. Res. Commun. *200*, 1484–1490.

Yang, J., Jan, Y.N., and Jan, L.Y. (1995). Control of rectification and permeation by residues in two distinct domains in an inward rectifier K^+ channel. Neuron *14*, 1047–1054.